CONTRIBUTION OF THREE-PARTICLE STATES TO THE EQUATION FOR THE SPECTRAL FUNCTIONS

V. N. GRIBOV and I. T. DYATLOV

Physico-technical Institute, Academy of Sciences, U.S.S.R.

Submitted to JETP editor December 7, 1961

J. Exptl. Theoret. Phys. (U.S.S.R.) **42**, 1268-1277 (May, 1962)

For a certain class of perturbation theory diagrams, containing three-particle intermediate states, we study the problem of expressing the spectral function $\rho(s, t)$ in terms of the absorptive parts of the subdiagrams that comprise the given diagram.

1. INTRODUCTION

IN the previous paper [1]* we have obtained an expression for the Mandelstam function $\rho(s, t)$ for the simplest class of perturbation theory diagrams, that contained a three-particle intermediate state (Fig. 1). This spectral function was represented in the form of an integral over five delta functions, corresponding to all the internal lines of the diagram. The region of integration over the variables not restricted by the delta functions turned out to be rather complicated and complex.

In the present work we shall show that also for the more involved class of diagrams (see Fig. 3), which correspond to the dependence of the amplitudes A_1 and A_2 (see Fig. 2) on two invariants, the rule [2] is valid according to which the spectral function for the diagram is obtained by replacing the Feynman denominators in a number of lines by delta functions. The region of integration over variables not restricted by the delta functions turns out to be similar to the region of integration for the diagram of Fig. 1. In the method chosen by us this region depends on the analytic properties of A_1 and A_2 as functions of all their variables.

However, for the diagrams of the type of Fig. 3 we shall show that the region of integration can be made independent of the properties of the amplitude as far as its dependence on s_{57} and s_{67} (see Secs. 2 and 3) is concerned. Moreover, we shall show that for these diagrams the corresponding function $\rho^{(3)}(s, t)$ can be expressed in the form of a certain integral over the absorptive parts of the amplitudes A_1 and A_2, taken over one of the variables of the type of momentum transfer (t_{15}, t_{35}, etc.). Consequently, the three-particle intermediate state in the unitarity condition contributes to $\rho(s, t)$ in the form of an integral fully analogous to that introduced by Mandelstam [3] for the contribution to $\rho(s, t)$ from a two-particle state. This allows us to formulate in Sec. 4 the idea of "partitions" for the calculation of $\rho(s, t)$ for an arbitrary diagram.

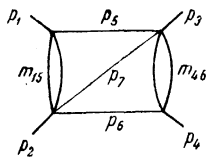

FIG. 1

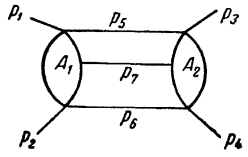

FIG. 2

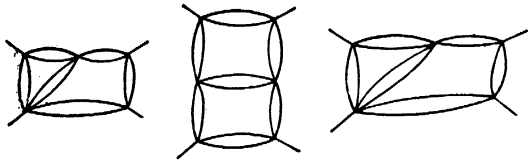

FIG. 3

However the problem of determining the entire region of integration in the case of the three-particle contribution remains open. It can be solved only after making a study of the analytic properties of the general five-point function when all its variables are varied simultaneously. It should be noted that for the calculation of $\rho(s, t)$ it is not necessary to have a knowledge of the analytic properties in the entire range of variation of the variables, it being sufficient to have this knowledge in a certain limited region in which the integration in the unitarity condition is carried out (continued in the momentum transfer t). Apparently, although it is true that the analytic properties of the amplitude with five or more external particles are quite involved, their behavior in the regions needed for the unitarity condition is such that the Mandelstam representation for the scat-

*In what follows we make use of the notation of [1], cited as I.

tering amplitude holds. The example analyzed in the present paper confirms this possibility.

2. SKELETON DIAGRAMS. THE INDEPENDENCE OF $\rho^{(3)}(s, t)$ OF THE SINGULARITIES IN s_{57}

From among all the diagrams with three-particle intermediate states (Fig. 2) we shall study only those represented in Fig. 3. For them the unitarity condition in any channel has a two-particle or three-particle structure, because if we express the subdiagrams of which these diagrams are composed in the form of dispersion integrals, they will turn out to be equivalent to the diagrams of Fig. 4 integrated with some weight over the masses of the virtual particles.

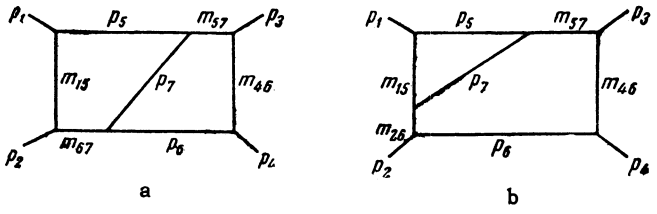

FIG. 4.

For example the contribution of the diagram pictured in Fig. 3b can be obtained from the diagram pictured in Fig. 4a by integration over the masses m_5, m_6, m_{57}, and m_{67} and the replacement of s by t. Diagrams of any other type give necessarily an effective contribution also to the four-particle unitarity relation in at least one channel. It may be that this is precisely the reason why their investigation is most involved and requires significant modifications in comparison with I.

We shall study the contribution to the absorptive part of the diagrams in Fig. 4 due to the three-particle intermediate state (the particles with momenta p_5, p_6, p_7), which will be referred to as the three-particle absorptive part. The contribution from two-particle intermediate states (p_{57}, p_6) and (p_5, p_{67}) (two-particle absorptive parts) can be easily investigated by the method proposed by Mandelstam.[3] If the masses of the internal and external particles are such that all the internal parts of the diagrams in Fig. 4 are normal then the two-particle contributions will give rise to the usual Karplus curves $t = t_N(s)$ with the asymptotes $s = (m_5 + m_{67})^2$ or $s = (m_{57} + m_6)^2$ and $t = (m_{15} + m_7 + m_{46})^2$ for Fig. 4a and $s = (m_{57} + m_6)^2$, $t = (m_{46} + m_{26})^2$ and $t = (m_{15} + m_7 + m_{46})^2$ for Fig. 4b. For them the function $\rho^{(2)}(s, t)$ is expressed in terms of the absorptive parts of the initial and final amplitudes in the unitarity relation [Eq. (I.15)].

The three-particle absorptive part with the intermediate state (p_5, p_6, p_7) may be written in the form of integrals analogous to Eqs. (I.20) and (I.21). For the diagram of Fig. 4a we have (with t in the physical region)

$$A_1^{(3)}(s, t) = \frac{1}{32(2\pi)^3} \int_{(m_5+m_7)^2}^{(\sqrt{s}-m_6)^2} ds_{57} \int \frac{dt_{26} f(s_{57}, t_{26}) \vartheta(1 - z_{26}^2)}{\sqrt{K(t, t_{26}, s_{57})}\,(s_{57} - m_{57}^2)}, \quad (1)$$

$$f(s_{57}, t_{26}) = \int \frac{ds_{67} \vartheta(1 - z_{56}^2)}{\sqrt{K(t_{26}, s_{67}, s_{57})}\,(s_{67} - m_{67}^2)}. \quad (2)$$

For the diagram of Fig. 4b $(s_{67} - m_{67}^2)^{-1}$ is replaced by $(t_{26} - m_{26}^2)^{-1}$. The definitions of all quantities are given in I. It is clear that the method used in I can be applied without any changes to the diagrams now being considered. The difference consists of the presence of additional poles in the variables s_{57} and s_{67} (or t_{26}). As in I we study the singular curves of the integral (1) in the s_{57} and t_{26} plane. They differ depending on whether $m_{15}^2 < (m_1 + m_5)^2$ or $m_{15}^2 > (m_1 + m_5)^2$.

a) For the case $m_{15}^2 < (m_1 + m_5)^2$ the singular curves are shown in Fig. 8 of I. To the pole $s_{57} = m_{57}^2$ corresponds a straight line parallel to the abscissa axis. When analytically continuing in t, the integration over s_{57} and t_{26} in Eq. (1) is carried out in the region LMB_tA_t, until the curve $t_{26}^-(t)(A_tB_t)$ (I.24) reaches the point E, at which the curve of singularities of the function $f(s_{57}, t_{26})$ – $t_{26}^{(1),(2)}$ (curve DEC) (I.23) touches the border of the region of integration over s_{57}.

For larger values of t there appears an additional region of integration D_tA_tE, which after passing through the singular point $t = t(s)$ goes out into the complex planes of s_{57} and t_{26} (see Figs. 5 and 6).

If $m_{57}^2 > (m_5 + m_7)^2$ then the pole $s_{57} = m_{57}^2$ will for sufficiently large s necessarily fall in the physical region of the variable s_{57}: $(m_5 + m_7)^2 < m_{57}^2 < (\sqrt{s} - m_6)^2$. The integral (1) will become complex for arbitrary t. However for that same s the contribution to the imaginary part of the

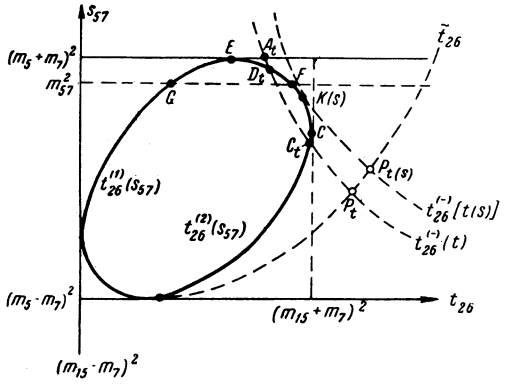

FIG. 5

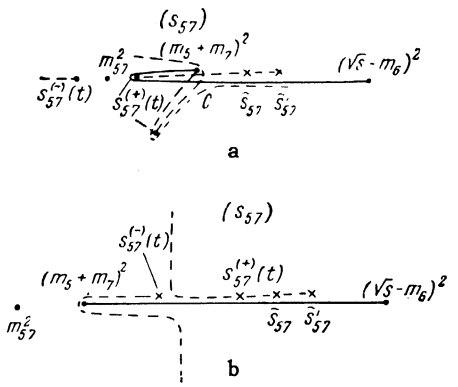

FIG. 6

diagrams of Fig. 4 comes not only from the three-particle intermediate state (p_5, p_6, p_7), but also from the two-particle state $(p_{57}, p_6; p_{57}^2 = m_{57}^2)$, and for the diagram of Fig. 4a also from the state $(p_{67}, p_5; p_{67}^2 = m_{67}^2)$.

The sum of the absorptive parts, corresponding to all possible intermediate states in the channel for which $s = (p_1 + p_2)^2$ is the energy, gives for $t < 0$ the imaginary part of the diagrams in Fig. 4 and is a real quantity. Consequently the imaginary part in the three-particle absorptive part, Eq. (1), should be compensated by the imaginary parts of the two-particle absorptive parts. It is easy to show that this is indeed the case. For the diagram of Fig. 4a the imaginary part of the integral (1) is for $t < 0$ equal to

$$\frac{-i\pi}{(2\pi)^3}\int d^4p_6 d^4p_{57}\delta^{(4)}(p_{57}+p_6-p_1-p_2)\,\delta(p_{57}^2-m_{57}^2) \times \delta(p_6^2-m_6^2)\,\frac{A_d}{t_{46}-m_{46}^2}, \tag{3}$$

$$A_d = \frac{1}{2(2\pi)^2}\int d^4p_5 d^4p_7\delta^{(4)}(p_{57}-p_5-p_7) \times \frac{\delta(p_5^2-m_5^2)\,\delta(p_7^2-m_7^2)}{(t_{15}-m_{15}^2)(s_{67}-m_{67}^2)}; \tag{4}$$

here A_d is the decay absorptive part[4] of the left quadrangle in the diagram of Fig. 4a.

On the other hand if we substitute into the two-particle absorptive part (p_{57}, p_6) in place of the right and left parts of the diagram the dispersion representations in the variables t_{26} and t_{46} we shall find, having made use of the representation for a quadrangle with an unstable particle,[4] that the imaginary part of $A_1^{(2)}(s, t)$ is for $t < 0$ equal to the quantity (3) taken with a minus sign. Such a cancellation takes place for all t. Consequently the decay absorptive parts of the internal parts of the diagram do not contribute to $\rho(s, t)$ for the diagram as a whole and have no effect on the position of its singularities.

If $m_{57}^2 < (m_5 + m_7)^2$, but the quadrangle with the external mass m_{57} that appears in the diagram of Fig. 4a (or the triangle in the diagram of Fig. 4b) has an anomalous singularity, then the pole $s_{57} = m_{57}^2$ will for some values of s fall within the region of integration $D_t A_t E$, which arises when the integral (1) is continued in t. Indeed, the straight line representing the pole intersects in this case the curves $t_{26}^{(1),(2)}$ in the points F and G, which lie higher than the point C [the maximum of the curve $t_{26} = t_{26}^{(2)}(s_{57})$ (see Fig. 5)]. The three-particle singularity $t = t(s)$ comes about when t is such that the points D_t and C_t coincide and the curve $t_{26}^{(-)}(t)$ touches the curve $t_{26}^{(2)}(s_{57})$ at some point K(s); for larger values of t the integration over the region $D_t A_t E$ proceeds then with complex values for s_{57} and t_{26}.

Depending on s, the point K(s) may lie on the curve $t_{26}^{(2)}(s_{57})$ above, as well as below, the point F. For $s \sim (m_5 + m_6 + m_7)^2$ the point K(s) lies near the point E, as s increases it coincides with the point F at $s = s_F$, and tends to the point C as $s \to \infty$. When the point K(s) lies above the point F, the pole $s_{57} = m_{57}^2$ does not fall within the range of integration of the integral for $A_1^{(3)}(s, t)$ which then only has the usual three-particle singularity studied in I. When however K(s) lies below F the integral $A_1^{(3)}(s, t)$ develops an additional singularity at $t = t_A(s)$ (Fig. 7) that satisfies the condition

$$t_{26}^{(-)}(t_A, m_{57}^2, s) = t_{26}^{(2)}(m_{57}^2). \tag{5}$$

What has been said above corresponds in the complex s_{57} plane (see Fig. 6a) to the possibility that the singularities $s_{57}^{(\pm)}(t)$, equal to the ordinates of the points D_t and C_t, might coalesce with the contour of integration captured by the singularity $s_{57}^{(+)}(t)$ going off into the complex plane* before

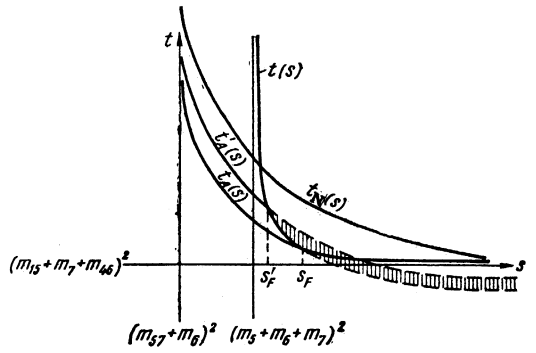

FIG. 7

*The details of the capture and the motion of the contour in the s_{57} plane and the appearance of the singularity t(s) are described in I.

(for $s < s_F$), as well as after (for $s > s_F$), intercepting the pole (see Fig. 7).

The imaginary part of $A_1^{(3)}$, due to the singularity (5), may be found in a way analogous to the calculation of $\rho(s, t)$ in I (see Appendix II in I). The desired imaginary part corresponds to the contour C (see Fig. 6) passing below or above (for $t = t_A \pm i\epsilon$) the pole $s_{57} = m_{57}^2$ and is equal to*

$$\pm \frac{1}{8(2\pi)^2} \int_{t_{26}^{(+)}(m_{57}^2)}^{t_{26}^{(-)}(t, m_{57}^2, s)} \frac{dt_{26}}{\sqrt{K(t, t_{26}, m_{57}^2)}} \times \int_{s_{67}^{(-)}}^{s_{67}^{(+)}} \frac{ds_{67}}{\sqrt{K(m_{57}^2, s_{67}, t_{26})(s_{67} - m_{67}^2)}}, \quad (6)$$

where $s_{67}^{(\pm)}$ are the roots of $K(m_{57}^2, s_{67}, t_{26}) = 0$ [see Eq. (I.22)]. The expression (6) differs from zero in the region $s > s_F$, $t_A(s) < t < t'_A(s)$, where $t'_A(s)$ is found from the equation

$$K(s_{57}, s_{67}, t_{26}, s)\big|_{s_{57}=m_{57}^2;\ s_{67}=m_{67}^2;\ t_{26}=t_{26}^{(-)}(t, m_{57}^2, s)} = 0. \quad (7)$$

At the point, Eq. (7), the integral over s_{67} becomes pure imaginary.

On the other hand, if one investigates according to Mandelstam the two-particle absorptive part corresponding to the intermediate state (p_{57}, p_6), one finds for the values of m_{57}^2 under consideration in addition to the normal two-particle Karplus curve $t = t_N(s)$ with the usual asymptotes two more anomalous curves. These curves are due to the anomalous addition in the dispersion relation for the box diagram [5] in the left part of Fig. 4a and are equal to the curves $t_A(s)$ and $t'_A(s)$, defined by Eqs. (5) and (7) (Fig. 7). The anomalous addition to the imaginary part of the two-particle absorptive part differs from zero in the region $t_A(s) < t < t'_A(s)$ and its amount is equal to the expression (6) taken with the opposite sign. Consequently, in the region $s > s_F$ the imaginary parts (6) of $A_1^{(3)}(s, t)$ and $A_1^{(2)}(s, t)$ cancel each other so that the internal anomalies give no contribution in this region.

Let us discuss in the s and t plane the Karplus curves for the diagram of Fig. 4a corresponding to the two- and three-particle states under consideration. From Fig. 5 it is easy to deduce the relative location of the Karplus curves, as shown in Fig. 7. For example in this case the curve $t_N(s)$ necessarily intersects the three-particle curve $t(s)$. Indeed, the equation for $t_N(s)$ is of the form

$$t_{26}^{(-)}(t, s_{57}, s)\big|_{s_{57}=m_{57}^2} = (m_{15} + m_7)^2. \quad (8)$$

But from Fig. 5 it is seen that for $s \sim (m_5 + m_6 + m_7)^2$ the condition (8) is satisfied before the three-particle singularity is produced [for $s \sim (m_5 + m_6 + m_7)^2$ the curve $t_{26}^{(-)}(t, s_{57}, s)$ is almost indistinguishable from a straight line parallel to the t_{26} axis], whereas for $s \to \infty$ [now $t_{26}^{(-)}(t, s_{57}, s)$ is a straight line parallel to the s_{57} axis] the situation is reversed. This means that the curves $t(s)$ and $t_N(s)$ intersect. In an analogous fashion the location of all the other curves may be determined. In particular the curve $t = t_A(s)$ necessarily touches the three-particle curve (the point $s = s_F$).

The anomalous additions contribute to $\rho(s, t)$ in the region between the curves $t = t_A(s)$ and $t = t'_A(s)$. Their cancellation occurs in the region shown dashed-in in Fig. 7. From the previous discussion it follows that this cancellation holds for $s > s_F$. It is easy to show that also in the region $t > t(s)$ and $s'_F < s < s_F$ (see Fig. 7) the curve $t = t'_A(s)$ is not singular and the anomalous contribution to the two-particle absorptive part is canceled for $t > t(s)$, if the contour in the s_{57} plane in Fig. 6 is drawn in an appropriate way. Consequently, the parts of the curves $t_A(s)$ and $t'_A(s)$ that are shown in Fig. 7 as dashed lines do not represent singularities for the diagram as a whole.

We have discussed the case when the left quadrangle of the diagram in Fig. 4a with the external mass m_{57} was anomalous. The same procedure can be followed when the quadrangle with the external mass m_{67} is anomalous. Then the contour over s_{67} in Eq. (2) (see I) reaches the value $s_{67} = m_{67}^2$ and an imaginary part appears in the integral (1) [for $t < t(s)$ and s larger than some s_N], which is canceled by the anomalous addition due to the two-particle absorptive part (due to the intermediate state consisting of particles with the momenta p_5, p_{67}). This can be verified easiest by writing $A_1^{(3)}(s, t)$ not in the form (1) and (2), but in terms of the variables s_{57}, s_{67}, t_{35} with the external integration carried out over s_{67}. In that case everything except for some relabeling reduces to the previously discussed case. On the other hand if the mass m_{67} is such that the quadrangle on the right-hand side of the diagram in Fig. 4a is normal, then the contour of integration in Eq. (2) does not reach the value $s_{67} = m_{67}^2$ in the region $t \leq t(s)$. For $t > t(s)$ it goes off into the

*We assume here that the mass m_{67}^2 is such that in the region $t < t(s)$ the pole $s_{67} = m_{67}^2$ of the integral (2) plays no role. This condition reduces to the requirement that the right-hand quadrangle of the diagram in Fig. 4a with the external mass m_{67} should not be anomalous. In that case $t'_A(s) > t_A(s)$ (see Fig. 7).

complex plane and the pole $s_{67} = m_{67}^2$ plays in the immediate vicinity of $t(s)$ no role in the expression for $A_1^{(3)}(s, t)$, except for the addition (6) in which we have taken it into account.

The reason for the cancellation discussed above is easy to understand. The condition that one of the internal quadrangles of the diagram in Fig. 4a be anomalous is not the same as the condition that the diagram as a whole be anomalous. Therefore the curves $t_A(s)$ and $t'_A(s)$, whose asymptotes lie at $t < (m_{15} + m_7 + m_{46})^2$, should not (in any event for large s) be singularities of the diagram, as indeed is the case. It is seen from here that the cancellation should occur also in the case when the anomaly of one of the quadrangles is due to an external mass (say, m_1), but the diagram as a whole remains, as before, not anomalous. A direct calculation confirms this conjecture. The case when the diagram as a whole is anomalous will not be considered.

Finally, if the mass m_{57} is such that the left quadrangle in Fig. 4a with the external mass m_{57} has no anomalous singularities, then the pole $s_{57} = m_{57}^2$ does not fall under the sign of the integral defining $A_1^{(3)}(s, t)$ and has no effect at all on $\rho^{(3)}(s, t)$.

b) The case $m_{15}^2 > (m_1 + m_5)^2$ corresponds precisely to the condition that the left-hand box in Fig. 4a have no anomalous singularities in t_{26} for arbitrary masses m_{57}. In that case the pole $s_{57} = m_{57}^2$ has, for $m_{57}^2 < (m_5 + m_7)^2$, no effect on $A_1^{(3)}(s, t)$, as also follows directly from Fig. 6b which represents the complex s_{57} plane with the singularities and the contour of integration for $m_{15}^2 > (m_1 + m_5)^2$. As regards the values $m_{57}^2 > (m_5 + m_7)^2$ and the pole in s_{67}, one finds that the situation is fully analogous to that given in this section and leads to the same results. It is obvious that the same investigation can be carried out in the same manner also for the diagram in Fig. 4b. Instead of the pole in s_{67} it contains a pole in t_{26}. The contribution to $\rho(s, t)$ due to the pole is easily written down and may be transformed into the Mandelstam form—a two-particle integral over the product of absorptive parts. This is obvious since this part of $\rho(s, t)$ corresponds to the contribution from two-particle intermediate states in the variable t. The absence of a pole in s_{67} simplifies the discussion for the case of an anomalous mass m_{57}.

Before passing to a discussion of these results we derive an expression for the contribution to $\rho(s, t)$ from the three-particle intermediate state, $\rho^{(3)}(s, t)$, for all values of t. The next section is devoted to this problem.

3. THE EXPRESSION FOR $\rho^{(3)}(s, t)$ FOR ARBITRARY VALUES OF t

Analogously to I, after passing the singular point $t = t(s)$ the amplitude $A_1^{(3)}(s, t)$ for the diagrams of Fig. 4 may be represented in the form

$$A_1^{(3)}(s, t) = \frac{1}{32(2\pi)^3} \int_C ds_{57} F(s_{57}, t, s) \frac{1}{s_{57} - m_{57}^2}, \tag{9}$$

$$F(s_{57}, t, s) = \int_{C'} \frac{dt_{26} f(s_{57}, t_{26})}{\sqrt{K(t, t_{26}, s_{57})}}. \tag{10}$$

The position of the contours C and C′ relative to the singularities of the integrands for the path $t \to t(s) + i\epsilon$ is shown in Figs. 6a and 8a for the case $m_{15}^2 < (m_1 + m_5)^2$, and in Figs. 6b and 8b for the case $m_{15}^2 > (m_1 + m_5)^2$. The contour C′ in Fig. 8, which defines the function $F(s_{57}, t, s)$, is shown for values of s_{57} near $(\sqrt{s} - m_6)^2$. Values of $F(s_{57}, t, s)$ for other s_{57} that enter the integral (9) are obtained by analytic continuation of Eq. (10) in s_{57}, with the path relative to the singularities of s_{57} specified by the rules indicated in Fig. 6. In that figure we show the change in the position of the singularities of $F(s_{57}, t, s)$ as t is increased.

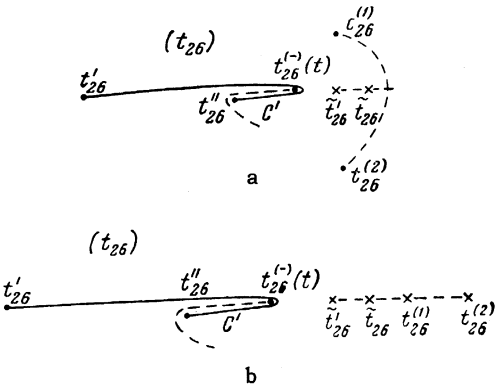

FIG. 8

If $\rho^{(3)}(s, t) = \mathrm{Im}\, A_1^{(3)}(s, t)$ is calculated with the help of Eqs. (9) and (10) then in the immediate vicinity of the singular point $t = t(s)$ one obtains formulas analogous to Eqs. (I.28) and (I.31), with the same region of integration. As was indicated in I, if t is further increased the region of integration for $\rho(s, t)$ of the diagram of Fig. 1 changes as compared to the Eqs. (I.28) and (I.31), because a new singularity of the function $f(s_{57}, t_{26})$, namely $\tilde{t}_{26} = (\sqrt{s_{57}} + m_1)^2$, starts to play a role. We shall now discuss in detail the problems that arise with the appearance of this singularity since it is responsible for the basic differences that appear for the diagrams of Fig. 4 as compared with the diagram of Fig. 1.

Let us consider the diagram of Fig. 1. The singularity $\tilde{t}_{26}$, shown in Fig. 8, will for some value of $t = \tilde{t}$ coincide with $t_{26}^{(-)}(t) = t_{26}^{(-)}(t, s_{57}, s)$ which results in the appearance of a new singularity of $F(s_{57}, t, s)$ in the s_{57} plane ($\tilde{s}_{57}$ in Fig. 6). This singularity appears in the s_{57} plane when $t = \tilde{t}$, having passed from the second sheet of the function $F(s_{57}, t, s)$ through the cut joining the singularities $s_{57}^{(+)}(t)$ and $s_{57}^{(-)}(t)$. Because the singularity $\tilde{s}_{57}$ appears through a cut whose position is well defined relative to the contour of integration C no new ambiguities are produced by it, and therefore $A_1^{(3)}(s, t)$ has no singularity at the point $t = \tilde{t}$. But the determination of the imaginary part of $A_1^{(3)}(s, t)$ changes from that point on.

The point $\tilde{s}_{57}$ is found from the equation

$$t_{26}^{(-)}(t, s_{57}, s) = (\sqrt{s_{57}} + m_1)^2. \qquad (11)$$

For the sake of definiteness let $m_{15}^2 < (m_1 + m_5)^2$. Then $\tilde{s}_{57}$ is the ordinate of the point P_t, Fig. 5. One can verify directly that the point $\tilde{s}_{57}$ is not a singular point for the branch of the function $F(s_{57}, t, s)$, defined on that side of the $s_{57}^{(+)}(t)$—$s_{57}^{(-)}(t)$ cut which contains the point $(m_5 + m_7)^2$. As soon as the point $\tilde{s}_{57}$ reaches the point $(m_5 + m_7)^2$ it appears in the s_{57} plane, since for the branch of the function $F(s_{57}, t, s)$, defined on the other side of the cut, $\tilde{s}_{57}$ is already a singularity. $\rho^{(3)}(s, t)$ receives a new addition to (I.31) in the form of the integral

$$\Delta\rho^{(3)}(s, t) = \frac{1}{32(2\pi)^3} \int_{(m_5+m_7)^2}^{\tilde{s}_{57}} ds_{57}\, \mathrm{Im}\, F(s_{57}, t, s). \qquad (12)$$

$\Delta\rho$ may be obtained in an analogous manner also in the case $m_{15}^2 > (m_1 + m_5)^2$.

One must take into account for the diagrams of Fig. 4 that as the point $\tilde{t}_{26} = (\sqrt{s_{57}} + m_1)^2$ is approached the root $s_{67}^{(+)}(t_{26}, s_{57}, s)$, having captured the contour of integration in the integral (2), goes off to $-\infty$ and then for $\tilde{t}_{26} > (\sqrt{s_{57}} + m_1)^2$ returns from $+\infty$ along the real axis. In essence, in its motion it traverses all values of s_{67} and consequently the pole $s_{67} = m_{67}^2$ will affect $A_1^{(3)}(s, t)$ of the diagram shown in Fig. 4a, resulting in the singularities $\tilde{t}'_{26}$ in the t_{26} plane (Fig. 8) and $\tilde{s}'_{57}$ (Fig. 6). These singularities are of the same nature as $\tilde{t}_{26}$ and $\tilde{s}_{57}$ and they change the determination of $\rho^{(3)}(s, t)$ as compared with the Eqs. (I.28), (I.31), and (12). The new addition to $\rho^{(3)}(s, t)$ will already be of a different nature than the remaining contributions to $\rho(s, t)$ (we do not write it out here since the concrete form of the diagrams in Fig. 4 is of no interest).

Indeed, both the expression (I.28) or (I.31) and (12) can be written in the form of an integral over a certain (complex) region over the absorptive parts of the five-point amplitudes, appearing in the left and right sides of the diagrams in Fig. 4 (A_1 and A_2 in Fig. 2). At that only absorptive parts of the five-point functions taken in one variable of the momentum transfer type (usual "jump") enter into the integrals of the type of Eqs. (I.28), (I.31), and (12). In that sense they are no different from the expression for the two-particle contribution $\rho^{(2)}(s, t)$ derived by Mandelstam [3] [see Eq. (I.15)]. The new addition, beside absorptive parts of the five-point functions taken in one variable, will contain an absorptive part taken in two variables consecutively (double "jump") (t_{15} and s_{67} for the diagram of Fig. 4a).

An analogous investigation in other variables—t_{35}, s_{57}, s_{67} —would in a certain sense give rise to the "inverse" result: the singularity in s_{67} plays no role in the determination of $\rho^{(3)}(s, t)$ (just like s_{57} in Sec. 2), whereas the singularity in s_{57} does contribute. This, of course, implies no contradiction since a given integral may be expressed in terms of integration over a variety of contours in a many-dimensional complex space, all of them yielding the same value. In particular, for the diagrams of Fig. 4 we could eliminate the additions to $\rho(s, t)$ that contain double "jumps" of the five-point functions by performing the integration for $A_1^{(3)}(s, t)$ in Eq. (9) for $t > t(s)$ along complex values of s_{57}, having deformed the contour C into the complex plane. Then the region of integration for the diagrams of Fig. 4 would differ in no way from the region of integration for the diagram of Fig. 1, which may be also deformed in the same way. On the other hand that region would not involve the pole $s_{67} = m_{67}^2$ for any value of t. In that case $\rho^{(3)}(s, t)$ would be expressed solely in terms of the usual absorptive parts of the five-point functions; in this sense the results of this section confirm the results of the previous one, since it was shown in Sec. 2 that all contributions to $\rho(s, t)$ that are not in the form of integrals over the usual absorptive parts (except for a part of the two-particle contribution) mutually cancel and do not contribute to ρ. This makes it possible to formulate the "partition" rule (see below).

4. CONCLUSION

It thus appears that it is possible to write for the contribution to $\rho(s, t)$ from the three-particle intermediate state a formula analogous to the Mandelstam formula for the two-particle contribution to ρ. According to it $\rho(s, t)$ is expressed in terms of the absorptive parts of the five-point

functions A_1 and A_2 (Fig. 2), taken over variables of the momentum transfer type $(t_{15}, t_{26}, t_{35}, t_{46})$ and integrated over a certain complex region of its arguments. By analytic changes of this region other formulas may be obtained for $\rho(s, t)$, containing in addition to the usual absorptive parts of the five-point functions also absorptive parts in two variables, etc. The nature of this region is not known to us in the general case, but apparently it differs significantly from the region derived for the diagrams of Fig. 1 or Fig. 4, since even the inclusion of singularities depending simultaneously on two variables (for example, t_{15} and s_{46}) results in a change of the contour of integration in the variables of the type of the mass m_{15}^2.

In the absence of singularities due to anomalies of internal parts of the diagrams [of the type $t_A(s)$ and $t'_A(s)$, Fig. 7], one could obtain $\rho(s, t)$ for an arbitrary diagram with four external lines by dividing the diagram into four parts by means of two partitions applied in all possible ways such that each part contains one and only one external line. Then those lines of the diagram that are traversed by the border of the partition are replaced by delta functions of $p_i^2 - m_i^2$ and an integration is carried out over a certain, generally speaking complex, region of the invariant variables, having first multiplied by a factor easily obtainable from the unitarity condition. The presence of anomalies results in the appearance of contributions to $\rho(s, t)$, expressible not in terms of the usual jumps of the amplitudes taken in one variable, as one would obtain according to the "partition" rule, but in terms of double, etc., jumps. But, apparently, these may be eliminated by deforming the contour of integration over the internal variables, just as we have done it for $\rho^{(3)}(s, t)$ for the diagrams of Fig. 4 (Sec. 3). Since in any event the region of integration for the general case has not been determined by us, within this reservation the "partition" rule turns out to be valid.

[1] V. N. Gribov and I. T. Dyatlov, JETP **42**, 196 (1962), Soviet Phys. JETP **15**, 140 (1962).

[2] R. E. Cutkosky, J. Math. Phys. **1**, 429 (1960).

[3] S. Mandelstam, Phys. Rev. **112**, 1344 (1958).

[4] Gribov, Danilov, and Dyatlov, JETP **41**, 1215 (1961), Soviet Phys. JETP **14**, 866 (1962).

[5] Gribov, Danilov, and Dyatlov, JETP **41**, 924 (1961), Soviet Phys. JETP **14**, 659 (1962).

Translated by A. M. Bincer
209